ELSEVIER

Journal of Nuclear Materials 299 (2001) 219–226

journal of nuclear materials

www.elsevier.com/locate/jnucmat

The structures of two sodium uranyl compounds relevant to nuclear waste disposal

Yaping Li, Peter C. Burns *

Department of Civil Engineering and Geological Sciences, University of Notre Dame, 156 Fitzpatrick, Notre Dame, IN 46556-0767, USA

Received 18 June 2001; accepted 12 September 2001

Abstract

Single crystals of two sodium uranyl phases, $Na_2[(UO_2)_3O_3(OH)_2]$ and $Na_4(UO_2)_2(Si_4O_{10})_2(H_2O)_4$ (designated NAUOH and NAURSI, respectively), were hydrothermally synthesized. Na uranyl oxyhydroxide (NAUOH) is monoclinic, space group $P2_1/n$, $a = 0.70476(3)$ nm, $b = 1.14126(6)$ nm, $c = 1.20274(6)$ nm, $\beta = 90.563(1)°$, $V = 0.96733(8)$ nm^3. The structure of NAUOH was solved by direct methods and refined on the basis of F^2 for 4027 unique reflections measuring using Mo Kα X-radiation and a CCD-based Smart APEX detector. The agreement index ($R1$) is 2.7%, calculated using 2955 unique observed reflections ($|F_o| \geqslant 4\sigma_F$), and the goodness-of-fit is 0.68. The structure contains uranyl pentagonal bipyramids that share vertices and edges, forming sheets parallel to (0 1 0). The sheets are linked by double chains of Na polyhedra located in the interlayer. NAUOH is a Na analogue of the mineral compreignacite, and may correspond to the Na uranyl oxide hydrate formed in studies of the oxidative dissolution of spent nuclear fuel. The phase $Na_4(UO_2)_2(Si_4O_{10})_2(H_2O)_4$ (NAURSI) is the Na analogue of $KNa_3(UO_2)_2(Si_4O_{10})_2(H_2O)_4$, which was found as an alteration phase on hydrothermally treated actinide-bearing borosilicate waste glass. It is monoclinic, space group $C2/m$, $a = 1.2770(1)$ nm, $b = 1.3610(1)$ nm, $c = 0.82440(8)$ nm, $\beta = 119.248(2)°$, $V = 1.2501(2)$ nm^3. The structure of NAURSI was solved by direct methods and refined on the basis of F^2 for 1483 unique reflections measured with Mo Kα X-radiation and a CCD-based Smart 1 K detector. The agreement index ($R1$) is 1.9%, calculated using 1333 unique observed reflections ($|F_o| \geqslant 4\sigma_F$), and the goodness-of-fit is 1.08. The structure is based on a uranyl silicate framework, with Na cations and H_2O groups located in interstitial sites. The structure is closely related to that of $KNa_3(UO_2)_2(Si_4O_{10})_2(H_2O)_4$.

1. Introduction

Safe disposal of nuclear waste in a geological repository involves unique scientific and engineering challenges owing to the very long-lived radioactivity of the waste. A repository must retain a variety of radionuclides that have vastly different chemical characters for thousands of years. Most of the radioactivity that will be housed in the proposed repository at Yucca Mountain, NV, USA, will be associated with spent nuclear fuel, much of which is derived from commercial reactors. Safe disposal of spent fuel requires a detailed knowledge of its long-term behavior under repository conditions, as well as the fate of radionuclides released from the spent fuel as waste containers are breached.

Natural analogue studies of the mineral uraninite, UO_{2+x} (an analogue for UO_2 in spent fuel) [1,2], as well as several laboratory-scale simulations [3–8], confirm that spent fuel is unstable under the moist, oxidizing conditions expected in the proposed repository at Yucca Mountain. Once containers are breached, alteration of the spent fuel may be rapid, with the most abundant alteration products being uranyl (U^{6+}) phases. Many of

* Corresponding author. Tel.: +1-219 631 7380; fax: +1-219 631 9236.

E-mail address: pburns@nd.edu (P.C. Burns).

0022-3115/01/$ - see front matter
PII: S0022-3115(01)00702-4

the uranyl phases can persist for thousands of years, as demonstrated by studies of natural analogues [9]. It is likely that uranyl phases forming due to the alteration of spent fuel will incorporate many of the radionuclides contained in the spent fuel [10–15], potentially having a profound impact upon the mobility of the radionuclides. An understanding of the impact of incorporation of radionuclides into uranyl phases is essential to an understanding of the long-term performance of the geological repository.

Finch et al. [5] examined the alteration products of spent nuclear fuel subjected to oxidative corrosion in dripping groundwater at 90 °C. The experiments used two pressurized-water-reactor fuels, ATM103 and ATM106, which have burn ups of ~30 and ~45 MWd/kg-U, respectively [5]. The groundwater used, designated EJ-13, was from well J-13 at the Yucca Mountain site, and was reacted with crushed Tonopah Springs tuff at 90 °C for 80 days. EJ-13 contains more Na and Si than J-13 water, with Na and Si concentrations of 46.5 and 34.4 μg/ml, respectively [3]. Tests involving weekly injection of 0.15 ml of EJ-13 water onto the spent fuel resulted in the formation of a novel Na uranyl oxide hydrate after 4.1 and 5.2 years [5]. However, insufficient quantities of material were recovered for full characterization, and it was tentatively identified it as the Na analogue of compreignacite [5], a K uranyl oxide hydrate [16]. We have synthesized, and determined the structure of, the Na analogue of compreignacite (designated NAUOH), and report the results herein.

Investigations of the hydrothermal alteration products of actinide-bearing borosilicate waste glass, which is a proposed actinide waste form, led to the discovery of a novel uranyl silicate compound with composition $KNa_3(UO_2)_2(Si_4O_{10})_2(H_2O)_4$ [14]. This phase may form as an alteration product of borosilicate waste glass in the proposed repository at Yucca Mountain, and may significantly impact the mobility of specific radionuclides by incorporating them into its crystal structure [14]. We have successfully synthesized the structurally related Na analogue (designated NAURSI) of $KNa_3(UO_2)_2(Si_4O_{10})_2(H_2O)_4$, with composition $Na_4(UO_2)_2(Si_4O_{10})_2(H_2O)_4$, and report the crystal structure herein.

2. Experimental

2.1. Synthesis of NAUOH

Synthesis of NAUOH was done in a 23 ml Teflon-lined stainless steel Parr bomb. The reactants were a mixture of 0.313 g uranyl acetate (Alfa), 0.03 g $Na_2(CO_3)$ (Fisher), and 4 ml of ultrapure H_2O. The reaction vessel was heated to 230 °C for 4 days, and then cooled to room temperature. The reaction produced a high yield of yellow crystals of NAUOH as well as a minor amount of α-UO_3.

2.2. X-ray analysis of NAUOH

A single crystal of NAUOH was selected for data collection and mounted on a Bruker Platform three-circle goniometer with a Smart CCD (charge-coupled device) APEX detector; the crystal-to-detector distance was 4.5 cm. Data were collected using monochromatic Mo Kα X-radiation with frame widths of 0.3° in ω. The unit-cell dimensions of NAUOH (Table 1) were refined from 2655 reflections using least-squares techniques. A sphere of data was collected and the three-dimensional data were reduced using the Bruker program SAINT. The data were corrected for Lorentz, polarization and background effects. A semi-empirical absorption correction was applied based on equivalent reflections by modeling the crystal as an ellipsoid, and lowered the R_{int} of 1173 intense reflections from 11.9% to 3.6%. A total of 19 384 intensities was measured, of which 4027 were independent ($R_{int} = 6.4\%$), with 2955 classed as observed reflections ($|F_o| \geqslant 4\sigma_F$). Additional information pertinent to the data collection is given in Table 1.

2.3. Synthesis of NAURSI

Crystals of NAURSI were obtained by mixing 0.23g UO_3 (Johnson Matthey), 0.228 g $Na_2SiO_3 \cdot H_2O$ (Baker) and 4 ml ultrapure water. The reactants were heated in a 23 ml Teflon-lined stainless steel Parr bomb to 250 °C for 2 days, and then cooled to room temperature.

2.4. X-ray analysis of NAURSI

Single crystal X-ray diffraction data for NAURSI were collected using a Bruker Platform three-circle goniometer with a 1K Smart CCD detector and a crystal-to-detector distance of 5 cm. Data were collected using monochromatic Mo Kα X-radiation and frame widths of 0.3° in ω. The unit-cell dimensions (Table 1) were refined from 2750 reflections using least-squares techniques. More than a hemisphere of data was collected. The three-dimensional data were reduced and corrected for Lorentz, polarization and background effects using the Bruker program SAINT. A semi-empirical absorption correction was done by modeling the crystal as a {0 1 0} plate, and reduced R_{int} of 2310 intense reflections from 14.9% to 4.1%. Reflections with a plate-glancing angle less than 3° were discarded. A total of 3537 intensities was collected, of which 1483 were independent ($R_{int} = 4.2\%$), with 1333 classed as observed reflections ($|F_o| \geqslant 4\sigma_F$). Additional information pertinent to the data collection is given in Table 1.

Table 1
Selected crystallographic data for NAUOH and NAURSI

	NAUOH	NAURSI
Structural formula	$Na_2[(UO_2)_3O_3(OH)_2]$	$Na_4(UO_2)_2(Si_4O_{10})_2(H_2O)_4$
Crystal size (mm^3)	$0.08 \times 0.05 \times 0.05$	$0.65 \times 0.26 \times 0.02$
Space group	$P2_1/n$	$C2/m$
a (nm)	0.70476(3)	1.2770(1)
b (nm)	1.14126(6)	1.3610(1)
c (nm)	1.20274(6)	0.82440(8)
β (°)	90.563(1)	119.248(2)
V (nm^3), Z	0.96733(8), 4	1.2501(2), 2
μ (mm^{-1})	50.2	13.5
ρ_{calc} (g/cm^3)	6.441	3.318
θ range for data collection	2.46–34.50°	2.36–28.28°
Reflections collected	19,384	3537
Independent reflections	4027 [$R_{(int)} = 0.0639$]	1483 [$R_{(int)} = 0.0417$]
Unique observed reflections	2955	1333
Refinement method	Full-matrix least-squares on F^2	Full-matrix least-squares on F^2
Goodness-of-fit on F^2	0.684	1.084
Final R indices [$I > 2\sigma(I)$]	$R1 = 0.0267$, $wR_2 = 0.0379$	$R1 = 0.0190$, $wR_2 = 0.0526$
R indices (all data)	$R1 = 0.0437$, $wR_2 = 0.0404$	$R1 = 0.0216$, $wR_2 = 0.0534$

$R1 = \sum(|F_o| - |F_c|)/\sum|F_o|$, $S = [\sum w(|F_o| - |F_c|)^2/(m-n)]^{1/2}$, for m observations and n parameters.

2.5. Structure solutions and refinements

Scattering curves for neutral atoms, together with anomalous-dispersion corrections, were taken from International Tables for X-Ray Crystallography, vol. IV [17]. The Bruker SHELXTL Version 5 system of programs was used for the determination and refinement of both structures.

Systematic absences indicated space group $P2_1/n$ for NAUOH, which was verified by solution of the structure by direct methods. The structure model included refined atomic coordinates, anisotropic-displacement parameters for all atoms, and a weighting scheme of the structure factors. It was refined on the basis of F^2 for all unique reflections, and gave a final $R1$ of 2.67%, calculated for the 2955 unique observed reflections, and a goodness-of-fit (S) of 0.68.

For NAURSI, the lack of systematic absence of reflections was consistent with space groups $C2$, $C2/m$ or Cm. The mean value of $|E^2 - 1| = 0.974$ indicated that the structure is likely centrosymmetric. It was solved in space group $C2/m$ by direct methods, which gave the positions of the U and Si atoms. Oxygen atom positions were located on difference-Fourier maps calculated after least-squares refinement of the model. Incorporation of a fully occupied Na(1) site, and partially occupied Na(2) and Na(3) sites into the model resulted in an R 1 of 4%. At this stage, it was noted that the anisotropic-displacement parameters for the Na(3) site were strongly asymmetric, and the site was replaced by a split-site model involving the Na(3A) and Na(3B) sites. This lowered $R1$ by ~2%. The unconstrained refined occupancies for the Na(2), Na(3A) and Na(3B) sites were 0.25(6), 0.52(2) and 0.34(2), respectively. Since Na(3A) has a symmetry equivalent site 0.204(2) nm away, occupancy of Na(3A) cannot excess 0.5, so it was fixed at 0.5 during subsequent cycles of refinement. The total occupancy of Na(2) and Na(3B) was constrained to be 0.5 to achieve charge balance. Strongly elongated anisotropic-displacement parameters also prompted a split-site model for the OW(9) site. The final structure model included all atomic positional parameters, the constrained total occupancy factors for Na(2) and Na(3B), and anisotropic-displacement parameters for all atoms. Refinement was done on the basis of F^2 for all unique reflections, and the final $R1$ was 1.90%, calculated for the 1333 unique observed reflections, with a goodness-of-fit of 1.08.

Further details concerning the structure refinements, final atomic positional and anisotropic-displacement parameters, and selected interatomic distances and angles for NAUOH and NAURSI are given in Tables 1–5.

3. Results

3.1. The structure of NAUOH

The structure of NAUOH contains three systematically distinct U^{6+} cations, each of which is part of an approximately linear $(UO_2)^{2+}$ uranyl ion (designated Ur), with U^{6+}–O_{Ur} bond lengths of ~0.18 nm, as is typically observed in uranyl compounds [18]. Each uranyl ion is further coordinated by five anions, arranged at the equatorial vertices of pentagonal bipyramids, with $\langle U(1)–\phi_{eq}\rangle$, $\langle U(2)–\phi_{eq}\rangle$ and $\langle U(3)–\phi_{eq}\rangle$ (ϕ: O^{2-} or OH^-,

Table 2
Atomic coordinates ($\times 10^4$) and anisotropic-displacement parameters ($\times 10^3$) for NAUOH

	x	y	z	U_{eq}[a]	U_{11}	U_{22}	U_{33}	U_{23}	U_{13}	U_{12}
U(1)	476(1)	2237(1)	1079(1)	7(1)	6(1)	9(1)	7(1)	0(1)	−1(1)	0(1)
U(2)	951(1)	2786(1)	4105(1)	8(1)	10(1)	9(1)	5(1)	0(1)	0(1)	1(1)
U(3)	−4317(1)	2479(1)	2319(1)	8(1)	7(1)	10(1)	7(1)	0(1)	1(1)	0(1)
Na(1)	−7527(4)	5035(3)	2143(2)	21(1)	23(2)	21(2)	19(2)	−1(1)	0(1)	−1(1)
Na(2)	−2547(4)	5034(3)	734(3)	30(1)	32(2)	33(2)	24(2)	−1(2)	4(2)	−10(2)
O(1)	352(6)	693(4)	1346(4)	12(1)	13(2)	8(2)	15(2)	3(2)	4(2)	−1(2)
O(2)	768(7)	3793(4)	712(4)	18(1)	21(3)	15(3)	17(3)	4(2)	−4(2)	−1(2)
O(3)	1179(6)	4364(4)	3933(4)	13(1)	13(2)	11(2)	14(3)	3(2)	0(2)	−3(2)
O(4)	729(8)	1187(4)	4301(4)	24(1)	42(4)	10(3)	20(3)	−1(2)	−1(3)	−1(2)
O(5)	−4623(7)	3977(4)	1864(4)	16(1)	23(3)	11(2)	13(2)	4(2)	6(2)	4(2)
O(6)	−4228(7)	988(4)	2832(4)	18(1)	17(3)	17(3)	19(3)	2(2)	0(2)	2(2)
O(7)	−2605(6)	2256(4)	756(3)	16(1)	12(2)	24(3)	10(2)	−4(2)	−1(2)	8(2)
O(8)	2495(6)	2409(5)	2542(4)	21(1)	5(2)	47(4)	10(2)	−7(2)	−2(2)	0(2)
O(9)	−1206(6)	2697(4)	2740(4)	18(1)	10(2)	28(3)	15(2)	−5(2)	2(2)	−1(2)
OH(10)	46(6)	1799(4)	−861(4)	15(1)	17(2)	19(3)	8(2)	0(2)	1(2)	1(2)
OH(11)	−1299(6)	3210(4)	5523(4)	13(1)	13(2)	17(3)	10(2)	3(2)	−2(2)	1(2)

[a] U(eq) is defined as one third of the trace of the orthogonalized U_{ij} tensor.

Table 3
Atomic coordinates ($\times 10^4$) and anisotropic-displacement parameters ($\times 10^3$) for NAURSI

	x	y	Z	U_{eq}[a]	U_{11}	U_{22}	U_{33}	U_{23}	U_{13}	U_{12}
U(1)	2500	2500	0	11(1)	10(1)	14(1)	8(1)	2(1)	3(1)	0(1)
Si(1)	2286(1)	3881(1)	−3858(1)	10(1)	11(1)	8(1)	11(1)	1(1)	5(1)	0(1)
Si(2)	545(1)	2191(1)	−6284(1)	10(1)	8(1)	10(1)	11(1)	−2(1)	3(1)	0(1)
Na(1)	0	3649(2)	0	30(1)	31(1)	24(2)	40(2)	0	21(1)	0
Na(2)	0	1056(9)	0	20(3)	30(7)	16(6)	15(5)	0	10(5)	0
Na(3A)	908(9)	0	−4170(15)	52(2)	81(6)	28(4)	64(5)	0	49(5)	0
Na(3B)	1115(12)	0	−3050(20)	44(4)	38(7)	29(7)	59(9)	0	20(7)	0
O(1)	1894(3)	5000	−4628(5)	12(1)	13(2)	9(2)	12(2)	0	4(2)	0
O(2)	2413(3)	3754(2)	−1854(4)	24(1)	36(2)	20(2)	17(1)	6(1)	15(1)	3(2)
O(3)	1251(3)	3203(2)	−5424(4)	21(1)	19(1)	12(1)	24(2)	−5(1)	5(1)	−5(1)
O(4)	−474(3)	2357(2)	−8372(4)	19(1)	13(2)	26(2)	13(1)	0(1)	3(1)	0(1)
O(5)	0	1781(3)	−5000	17(1)	22(2)	14(2)	20(2)	0	14(2)	0
O(6)	2281(3)	3360(2)	1482(4)	20(1)	21(2)	23(2)	16(1)	−4(1)	8(1)	2(1)
O(7)	3544(2)	3670(2)	−3832(4)	19(1)	13(1)	15(2)	30(2)	−2(1)	11(1)	2(1)
OW(8)	312(5)	5000	−1642(7)	28(1)	30(3)	31(3)	24(2)	0	13(2)	0
OW(9A)	801(13)	0	−1290(20)	48(3)						
OW(9B)	990(20)	0	−410(30)	98(7)						

[a] U(eq) is defined as one third of the trace of the orthogonalized U_{ij} tensor.

ϕ_{eq}: equatorial ϕ) bond lengths of 0.2337, 0.2398 and 0.2370 nm, respectively. The uranyl polyhedra link by sharing equatorial edges and vertices, forming an α-U_3O_8-type sheet that is parallel to (0 1 0) (Fig. 1(a)). The α-U_3O_8-type sheet is common in uranyl oxide hydrate phases, and occurs in compreignacite $K_2[(UO_2)_3O_2(OH)_3]_2(H_2O)_7$ [16], becquerelite $Ca[(UO_2)_3O_2(OH)_3]_2(H_2O)_8$ [19], billetite $Ba[(UO_2)_3O_2(OH)_3]_2(H_2O)_4$ [19], protasite $Ba[(UO_2)_3O_3(OH)_2](H_2O)_3$ [19], agrinierite $K_2(Ca_{0.65}Sr_{0.35})[(UO_2)_3O_3(OH)_2]_2(H_2O)_5$ [20], masuyite $Pb[(UO_2)_3O_3(OH)_2](H_2O)_3$ [21], and richetite $M_xPb_{8.57}[(UO_2)_{18}O_{18}(OH)_{12}]_2(H_2O)_{41}$ [22], as well as a synthetic Cs uranyl oxide hydrate [23]. The Ur(2)ϕ_5 polyhedron is strongly distorted, with U(2)–ϕ_{eq} bond lengths ranging from 0.2223 to 0.2924 nm (Table 4). A similarly distorted uranyl pentagonal bipyramid occurs in the structure of billetite [19].

There are two unique Na cation sites in the structure of NAUOH, both of which are located in the interlayer regions between the sheets (Fig. 1(b)). Site occupancy refinement indicates each site is fully occupied by Na. The Na(1) and Na(2) sites are coordinated by 7 and 6 oxygen atoms, respectively, with $\langle$Na(1)–O$\rangle$ and $\langle$Na(2)–O$\rangle$ bond distances of 0.2525 and 0.2519 nm,

Table 4
Selected bond distances (nm) and angles (°) for NAUOH[a]

U(1)–O(1)	0.1794(4)	U(2)–O(3)	0.1820(4)	U(3)–O(5)	0.1807(5)
U(1)–O(2)	0.1842(5)	U(2)–O(4)	0.1847(5)	U(3)–O(6)	0.1811(5)
U(1)–O(7)	0.2202(4)	U(2)–O(7)b	0.2223(4)	U(3)–O(7)	0.2258(4)
U(1)–O(8)	0.2261(4)	U(2)–O(8)	0.2223(4)	U(3)–O(9)	0.2260(4)
U(1)–O(9)	0.2392(4)	U(2)–O(9)	0.2228(4)	U(3)–O(8)c	0.2267(4)
U(1)–O(10)	0.2402(4)	U(2)–OH(11)	0.2390(4)	U(3)–OH(10)d	0.2386(4)
U(1)–O(11)a	0.2429(4)	U(2)–OH(10)b	0.2924(5)	U(3)–OH(11)e	0.2679(4)
O(1)–U(1)–O(2)	174.9(2)	O(3)–U(2)–O(4)	179.1(2)	O(5)–U(3)–O(6)	174.7(2)
$\langle U(1)–O_{Ur}\rangle$	0.1818	$\langle U(2)–O_{Ur}\rangle$	0.1833	$\langle U(3)–O_{Ur}\rangle$	0.1809
$\langle U(1)–O_{eq}\rangle$	0.2337	$\langle U(2)–O_{eq}\rangle$	0.2398	$\langle U(3)–O_{eq}\rangle$	0.2370
Na(1)–O(5)	0.2402(5)	Na(2)–O(5)	0.2341(5)		
Na(1)–O(3)c	0.2469(5)	Na(2)–O(6)f	0.2384(6)		
Na(1)–O(1)f	0.2482(5)	Na(2)–O(4)e	0.2519(6)		
Na(1)–O(2)c	0.2524(6)	Na(2)–O(2)h	0.2536(5)		
Na(1)–O(4)f	0.2528(6)	Na(2)–O(4)f	0.2600(6)		
Na(1)–O(6)g	0.2533(6)	Na(2)–O(2)	0.2732(6)		
Na(1)–O(8)f	0.2736(6)	⟨Na(2)–O⟩	0.2519		
⟨Na(1)–O⟩	0.2525				

[a] $a=-x-1,-y+1,-z$; $b=x+1/2,-y+1/2$, $z+1/2$; $c=x-1,y,z$; $d=x-1/2,-y+1/2,z+1/2$; $e=x-1/2,-y+1/2$, $z-1/2$; $f=-x-1/2,y+1/2,-z+1/2$; $g=-x-3/2,y+1/2,-z+1/2$; $h=-x,-y+1,-z$.

Table 5
Selected bond distances (nm) and angles (°) for NAURSI[a]

U(1)–O(6)a	0.1809(3)	Si(1)–O(2)	0.1589(3)	Si(2)–O(4)	0.1587(3)
U(1)–O(6)	0.1809(3)	Si(1)–O(3)	0.1611(3)	Si(2)–O(3)	0.1609(3)
U(1)–O(2)	0.2257(3)	Si(1)–O(7)	0.1623(3)	Si(2)–O(7)d	0.1620(3)
U(1)–O(2)a	0.2257(3)	Si(1)–O(1)	0.1632(2)	Si(2)–O(5)	0.1623(2)
U(1)–O(4)b	0.2267(3)	⟨Si(1)–O⟩	0.1590	⟨Si(2)–O⟩	0.1610
U(1)–O(4)c	0.2267(3)				
O(6)a–U(1)–O(6)	180.0(2)	O(2)–Si(1)–O(3)	113.5(2)	O(4)–Si(2)–O(3)	110.0(2)
$\langle U(1)–O_{Ur}\rangle$	0.1809	O(2)–Si(1)–O(7)	111.7(2)	O(4)–Si(2)–O(7)d	110.6(2)
$\langle U(1)–O_{eq}\rangle$	0.2262	O(3)–Si(1)–O(7)	109.2(2)	O(3)–Si(2)–O(7)d	111.2(2)
		O(2)–Si(1)–O(1)	111.2(2)	O(4)–Si(2)–O(5)	111.8(1)
		O(3)–Si(1)–O(1)	104.3(2)	O(3)–Si(2)–O(5)	109.5(2)
		O(7)–Si(1)–O(1)	106.5(2)	O(7)d–Si(2)–O(5)	103.7(2)
		⟨O–Si(1)–O⟩	109.4	⟨O–Si(2)–O⟩	109.5
Na(1)–O(8)	0.2429(4)	Na(2)–OW(9A)	0.230(1)	Na(3A)–OW(9A)	0.245(2)
Na(1)–O(8)e	0.2429(4)	Na(2)–OW(9A)h	0.230(1)	Na(3A)–O(5)j	0.2630(6)
Na(1)–O(4)c	0.2460(4)	Na(2)–O(4)c	0.2469(9)	Na(3A)–O(5)	0.2630(6)
Na(1)–O(4)f	0.2460(4)	Na(2)–O(4)f	0.2469(9)	Na(3A)–O(7)k	0.2758(7)
Na(1)–O(6)g	0.2580(3)	Na(2)–O(7)a	0.2799(3)	Na(3A)–O(7)d	0.2758(7)
Na(1)–O(6)	0.2580(3)	Na(2)–O(7)i	0.2799(3)	⟨Na(3A)–ϕ⟩	0.265
⟨Na(1)–O⟩	0.2490	⟨Na(2)–ϕ⟩	0.252		
Na(3B)–OW(9B)	0.226(3)	Na(3B)–O(5)	0.2873(9)	Na(3B)–O(6)l	0.2874(9)
Na(3B)–O(5)j	0.2873(9)	Na(3B)–O(6)a	0.2874(9)	⟨Na(3B)–ϕ⟩	0.275

[a] $a=-x+1/2,-y+1/2,-z$; $b=x+1/2,-y+1/2,z+1$; $c=-x,y,-z-1$; $d=-x+1/2,-y+1/2,-z-1$; $e=-x,-y+1,-z$; $f=x,y,z+1$; $g=-x,y,-z$; $h=-x,-y,-z$; $i=x-1/2,-y+1/2,z$; $j=-x,-y,-z-1$; $k=-x+1/2,y-1/2,-z-1$, $l=-x+1/2,y-1/2,-z$.

respectively. The Na polyhedra share edges, forming polyhedral chains 2 polyhedra wide (Fig. 1(c)). The chains extend along [1 0 0] and provide linkage between the sheets of uranyl polyhedra.

3.2. Formula of NAUOH

All atoms in the structure of NAUOH are on general positions in space group $P2_1/n$. Of the 12 anions,

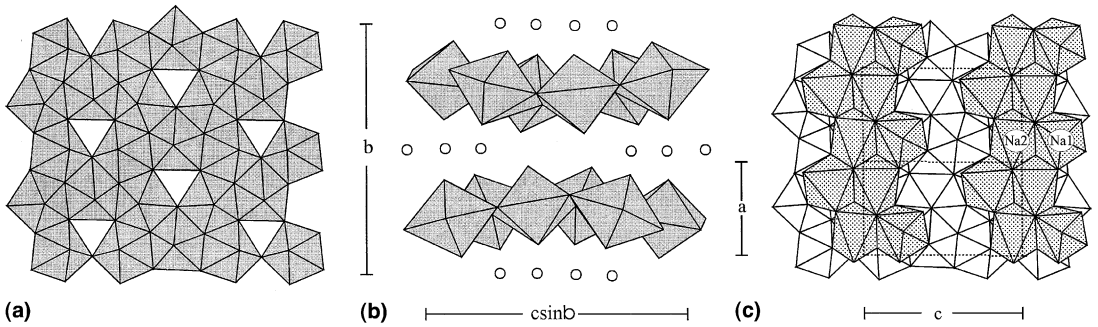

Fig. 1. Polyhedral representation of the structure of NAUOH. (a) The α-U_3O_8 sheet of uranyl pentagonal bipyramids projected along [0 1 0]. (b) The structure projected along [1 0 0]; open circles represent Na cations. (c) The structure projected along [0 1 0], with Na polyhedra shaded with dots.

Table 6
Bond-valence[a] (*v.u*) analysis for NAUOH

	U(1)	U(2)	U(3)	Na(1)	Na(2)	$\sum$
O(1)	1.64			0.16		1.80
O(2)	1.49			0.14	0.14, 0.08	1.85
O(3)		1.56		0.16		1.72
O(4)		1.47		0.14	0.14, 0.12	1.87
O(5)			1.60	0.20	0.23	2.03
O(6)			1.58	0.14	0.21	1.93
O(7)	0.75	0.71	0.66			2.12
O(8)	0.66	0.71	0.65	0.08		2.10
O(9)	0.51	0.70	0.66			1.87
OH(10)	0.50	0.18	0.51			1.19
OH(11)	0.47	0.51	0.29			1.27
$\sum$	6.02	5.84	5.95	1.02	0.92	

[a] Bond-valence parameters for U^{6+} from Burns et al. [18] and for Na^+ from Brese and O'Keeffe [27].

bond-valence analysis (Table 6) indicate there are 10 O^{2-} and 2 are $(OH)^-$ anions. The formula can thus be written as $Na_2[(UO_2)_3O_3(OH)_2]$, $Z = 4$, with the sheet constituents enclosed in square brackets.

3.3. The structure of NAURSI

The structure of NAURSI is closely related to that of $KNa_3(UO_2)_2(Si_4O_{10})_2(H_2O)_4$ [14]. Both structures contain identical sheets of vertex-sharing silicate tetrahedra (Fig. 2(a)) that are linked to uranyl square bipyramids, resulting in open frameworks with low-valence cations and H_2O groups located in interstitial sites (Fig. 2(b)). In the structure of NAURSI, there is a single symmetrically distinct U^{6+} cation that is strongly bonded to 2 oxygen atoms, giving an approximately linear $(UO_2)^{2+}$ uranyl ion with a $\langle U–O_{Ur}\rangle$ bond length of 0.1809 nm. The uranyl ion is coordinated by 4 atoms of O arranged at the equatorial vertices of a square bipyramid that is capped by the O_{Ur} atoms, with a $\langle U–O_{eq}\rangle$ bond length of 0.2262 nm. There are two symmetrically distinct Si cations that are tetrahedrally coordinated by O atoms, with $\langle Si(1)–O\rangle$ and $\langle Si(2)–O\rangle$ bond lengths of 0.1590 and 0.1610 nm, respectively (Table 5).

The structure of NAURSI contains 4 systematically distinct Na sites. The Na(1) site, which is fully occupied, is coordinated by 6 oxygen atoms with a $\langle Na(1)–O\rangle$ bond length of 0.2490 nm. The Na(2) site is 22.0(4)% occupied, and is coordinated by 4 oxygen atoms and $2H_2O$ groups, with a $\langle Na(2)–\phi\rangle$ bond length of 0.252 nm. The Na(3) site was modeled as a split site, designated Na(3A) and Na(3B), with a separation of ~0.08 nm. The Na(3A) and Na(3B) sites are 50% and 28.0(5)% occupied, respectively. Each of these sites is coordinated by 4 O atoms and one H_2O group, with $\langle Na(3A)–\phi\rangle$ and $\langle Na(3B)–\phi\rangle$ bond lengths of 0.265 and 0.275 nm, respectively (Table 5). There are three unique H_2O sites, OW(8), OW(9A) and OW(9B), with the half-occupied OW(9A) and OW(9B) sites separated by ~0.09 nm.

3.4. Formula of NAURSI

Based on the structure determination, the single unique U^{6+} cation is located on Wyckoff position *e* in space

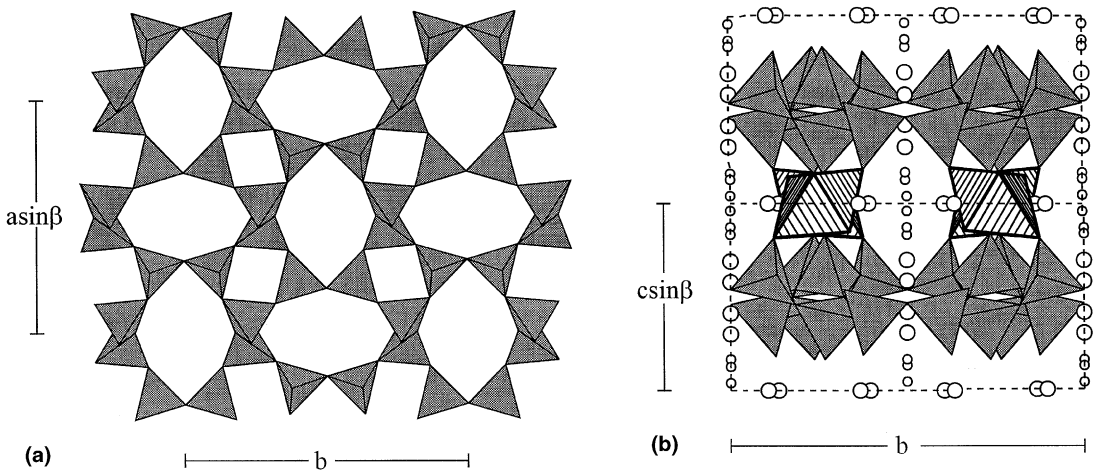

Fig. 2. Polyhedral representation of the structure of NAURSI. (a) Vertex-sharing sheet of Si tetrahedra projected along [0 0 1]. (b) Structure projected along [1 0 0]. The uranyl polyhedra are shown shaded with parallel lines, the Si tetrahedra are dark gray. The large and small open circles represent Na cations and H_2O groups, respectively.

group $C2/m$, giving $4U^{6+}$ atoms per unit cell. Both of the Si(1) and Si(2) sites are on general positions, giving 16 Si atoms per unit cell. The Na(1) and Na(2) sites are on positions g, and Na(3A) and Na(3B) are on positions i, giving a total of 8 Na atoms per unit cell. The O(1) site is on position i, O(5) on h, and O(2), O(3), O(4), O(6), and O(7) are on general positions, giving a total of 48 oxygen atoms per unit cell. The OW(8), OW(9A) and OW(9B) H_2O groups are on positions i, but OW(9A) and OW(9B) are only 50% occupied, resulting in $8H_2O$ groups per unit cell. The resulting formula of NAURSI is thus $Na_4(UO_2)_2(Si_4O_{10})_2(H_2O)_4$, $Z = 2$.

4. Discussion

Laboratory simulations have shown that a Na uranyl oxide hydrate with a morphology similar to compreignacite may be an important alteration phase of spent fuel in the proposed repository at Yucca Mountain [5]. We have successfully synthesized a phase that is a Na analogue of compreignacite, and that may be the phase found in studies of the oxidative dissolution of spent fuel. Although NAUOH has a sheet of uranyl polyhedra that is topologically identical to that in compreignacite, there are important differences in these two structures. The interlayer in NAUOH contains no H_2O, whereas compreignacite involves $7H_2O$ per formula unit [16]. In NAUOH the ratio of alkali metal contained in the interlayer to uranium in the sheets is 2:3, whereas in compreignacite it is 1:3. The sheets of uranyl polyhedra in NAUOH contain less H than in compreignacite, providing for charge balance associated with the increase in the amount of alkali metal in the interlayer. The distribution of $(OH)^-$ groups in the sheet of uranyl polyhedra in NAUOH is identical to that found in protasite [19] and agrinierite [20], and is one of 4 distinct distributions of $(OH)^-$ groups known for α-U_3O_8-type sheets of uranyl polyhedra [23].

Incorporation of Np into crystals of uranyl oxide hydrate (dehydrated schoepite) that formed on the surface of spent nuclear fuel has been reported [10]. If NAUOH forms as an alteration product of spent fuel, it may also incorporate Np, thereby potentially significantly impacting upon actinide mobility under repository conditions. The polyhedral geometries found for Np^{5+} in crystal structures are very similar to those found for U^{6+}, including the presence of a (NpO_2) neptunyl ion that is similar to the uranyl ion, although bond lengths are slightly longer in the case of Np [15]. Certainly, incorporation of Np^{5+} into the structure of NAUOH is permissible from the perspective of polyhedral geometries. However, a charge-balance mechanism is essential for incorporation of Np^{5+} in substitution for U^{6+}. The α-U_3O_8-type sheet of uranyl polyhedra is sufficiently flexible to permit additional hydration of an O atom that occurs at the equatorial vertices of three uranyl pentagonal bipyramids, as demonstrated by the occurrences of four distinct distributions of $(OH)^-$ in this sheet type [23]. Thus, a possible charge-balance mechanism is $Np^{5+}, (OH)^- \rightarrow U^{6+}, O$. It is likely that Np will be incorporated into the structure of NAUOH, although experimental verification is needed.

The structure of NAUOH is the first Na uranyl phase demonstrated to contain sheets of uranyl pentagonal bipyramids. Several synthetic high-temperature anhydrous Na uranyl compounds (Na_2UO_4, $Na_2U_2O_7$, Na_4UO_5, $NaUO_3$, Na_3UO_4, $Na_6U_7O_{24}$) have been documented in the system of UO_3–Na_2O [24]. Some of their structures, as well as that of clarkeite, ideally

$Na[(UO_2)O(OH)](H_2O)_{0-1}$ [25], are based on sheets of uranyl hexagonal bipyramids. A synthetic stoichiometric Na uranyl oxyhydroxide with a Na:U ratio of 1:3 has been synthesized, and its structure was predicted to contain sheets of uranyl pentagonal bipyramids [26], but this has not been confirmed.

The phase $KNa_3(UO_2)_2(Si_4O_{10})_2(H_2O)_4$ formed on hydrothermally altered actinide-bearing borosilicate waste glass (51S) that contained 9.30 and 1.36 wt.% Na_2O and K_2O, respectively [14]. Burns et al. [14] predicted that this phase may form due to alteration of glass under the conditions of the proposed repository at Yucca Mountain, and that it may significantly impact upon the release of radionuclides by their incorporation directly into its crystal structure. Owing to the high Na content of the rocks and water at Yucca Mountain, it is possible that NAURSI will form rather than $KNa_3(UO_2)_2(Si_4O_{10})_2(H_2O)_4$. However, our study has shown that these phases are very closely related, with structures that contain identical uranyl silicate frameworks. The structures differ only in the contents of the interstitial constituents, with one of the 4 sites that contain alkali cations in $KNa_3(UO_2)_2(Si_4O_{10})_2(H_2O)_4$ empty in the case of NAURSI. The interstitial cation sites in each structure involve partial occupancies, and in both cases the total interstitial cations per formula unit is 4. It is likely that solid solution may occur between these two phases.

Burns et al. [14] discussed potential incorporation mechanisms for radionuclides in the structure of $KNa_3(UO_2)_2(Si_4O_{10})_2(H_2O)_4$. Identical incorporation mechanisms should be possible for NAURSI, although experimental confirmation is needed.

Acknowledgements

This research was funded by the Environmental Management Sciences Program of the United States Department of Energy (DE-FG07-97ER14820).

References

[1] R.J. Finch, R.C. Ewing, J. Nucl. Mater. 190 (1992) 133.
[2] E.C. Pearcy, J.D. Prikryl, W.M. Murphy, B.W. Leslie, Appl. Geochem. 9 (1994) 713.
[3] D.J. Wronkiewicz, J.K. Bates, T.J. Gerding, E. Veleckis, B.S. Tani, J. Nucl. Mater. 190 (1992) 107.
[4] D.J. Wronkiewicz, J.K. Bates, S.F. Wolf, E.C. Buck, J. Nucl. Mater. 238 (1996) 78.
[5] R.J. Finch, E.C. Buck, P.A. Finn, J.K. Bates, Mater. Res. Soc. Symp. Proc. 556 (1999) 431.
[6] P.A. Finn, S.F. Wolf, R.A. Leonard, R.J. Finch, E.C. Buck, in: Seventh International Conference on the Chemistry and Migration Behavior of Actinides and Fission Products in the Geosphere, Incline Village, Lake Tahoe, NV, USA, September 26–October 1, 1999, Abstracts, vol. 7, 1999, p. 17.
[7] P.A. Finn, J.C. Hoh, S.F. Wolf, S.A. Slater, J.K. Bates, Radiochim. Acta 74 (1996) 65.
[8] E.C. Buck, D.J. Wronkiewicz, P.A. Finn, J.K. Bates, J. Nucl. Mater. 249 (1997) 70.
[9] R.J. Finch, J. Suksi, K. Rasilainen, R.C. Ewing, Mater. Res. Soc. Symp. Proc. 412 (1996) 823.
[10] E.C. Buck, R.J. Finch, P.A. Finn, J.K. Bates, Mater. Res. Soc. Symp. Proc. 506 (1998) 87.
[11] P.C. Burns, J. Nucl. Mater. 265 (1999) 218.
[12] P.C. Burns, R.J. Finch, F.C. Hawthorne, M.L. Miller, R.C. Ewing, J. Nucl. Mater. 249 (1997) 199.
[13] P.C. Burns, F.C. Hill, Can. Mineral. 38 (2000) 175.
[14] P.C. Burns, R.A. Olson, R.J. Finch, J.M. Hanchar, Y.J. Thibault, J. Nucl. Mater. 278 (2000) 290.
[15] P.C. Burns, R.C. Ewing, M.L. Miller, J. Nucl. Mater. 245 (1997) 1.
[16] P.C. Burns, Can. Mineral. 36 (1998) 1061.
[17] J.A. Ibers, W.C. Hamilton (Eds.), International Tables for X-ray Crystallography, IV, Kynoch, Birmingham, UK, 1994.
[18] P.C. Burns, R.C. Ewing, F.C. Hawthorne, Can. Mineral. 35 (1997) 1551.
[19] M.K. Pagoaga, D.E. Appleman, J.M. Stewart, Am. Mineral. 72 (1987) 1230.
[20] C.L. Cahill, P.C. Burns, Am. Mineral. 85 (2000) 1294.
[21] P.C. Burns, J.M. Hanchar, Can. Mineral. 37 (1999) 1483.
[22] P.C. Burns, Can. Mineral. 36 (1998) 187.
[23] F.C. Hill, P.C. Burns, Can. Mineral. 37 (1999) 1283.
[24] T.B. Lindemer, T.M. Besmann, J. Nucl. Mater. 100 (1981) 178.
[25] R.J. Finch, R.C. Ewing, Am. Mineral. 82 (1997) 607.
[26] P.D. Arocras, B. Grambow, Geochim. Cosmochim. Acta 62 (1998) 245.
[27] N.E. Brese, M. O'Keeffe, Acta Crystallogr. B 47 (1991) 192.